View metadata, citation and similar papers at core.ac.uk

brought to you by CORE

provided by Sheffield Hallam University Research Archive

Numerical Investigation of Dynamic Pipe-Soil Interaction on Electrokinetic-Treated Soft Clay Soil

JOSHUA, H.N. and KARA, Fuat

Available from Sheffield Hallam University Research Archive (SHURA) at:

http://shura.shu.ac.uk/25740/

This document is the author deposited version. You are advised to consult the publisher's version if you wish to cite from it.

Published version

JOSHUA, H.N. and KARA, Fuat (2020). Numerical Investigation of Dynamic Pipe-Soil Interaction on Electrokinetic-Treated Soft Clay Soil. Journal of Waterway, Port, Coastal and Ocean Engineering, 146 (1), 04019033-04019033.

Copyright and re-use policy

See http://shura.shu.ac.uk/information.html

Sheffield Hallam University Research Archive
http://shura.shu.ac.uk

NUMERICAL INVESTIGATION OF DYNAMIC PIPE-SOIL INTERACTION ON ELECTRO-KINETIC TREATED SOFT CLAY SOIL

Hakuri Nwen Joshua

PhD

School of Water, Energy and Environment,

Energy Theme, Cranfield University, MK43 0AL, UK

joshuahaku@yahoo.com

Fuat Kara (PhD)

Senior Lecturer

Mechanical Engineering Department

Sheffield Hallam University

fuat.kara@shu.ac.uk

ABSTRACT

Researchers have underscored the importance for a pipeline to safeguard against adverse effect resulting from its displacement in vertical, axial and lateral directions due to the low shear strength of the soil. Seabed may sometimes consist of soft or very soft clay soil with high water content and low shear strength. Dissipation of the water content from the soil void increases its effective stress with a resultant increase in the soil shear strength. Electro-kinetic (EK) concept has been applied to increase soil bearing capacity with barely any study conducted on it possible application on pipe-soil interaction. The need to explore more options merit further research. The EK process for the pipe-soil interaction consist of two main stages: electro-osmotic consolidation process and the dynamic analyses of the pipe-soil interaction. The present study numerically investigates the impact of EK treated soil on pipe-soil interaction over the non-EK process. Results of dynamic pipe-soil interaction on EK treated soil when compared with non-EK treated soil indicates a significant increase in the force required to displace a pipeline.

***KEYWORDS*:** Electro-kinetic, Electro-osmosis , Consolidation, Pore pressure, Effective Stress, Electrodes, Displacement, Submarines Pipeline.

INTRODUCTION

Subsea pipelines are subjected to harsh environmental conditions leading to their displacement in vertical, axial and lateral directions. Complex and expensive mitigating measures are currently being employed to keep the pipeline in place. An increase in soil shear strength does increase the frictional resistance against pipeline displacement. Electro-kinetic (EK) soil treatment process is applied to increase the strength of soil, however, little or no attention is given to EK process with

regard to pipe-soil interaction. The EK process consists of electro-osmotic consolidation followed by the dynamic pipe-soil interactions.

The strength of the soil can be improved by the electro-osmotic consolidation process. The application of electrical voltage induces movement of soil pore water from the anodes to cathodes (Al-Hamdan and Reddy 2008) with a resultant increase in the soil effective stress due to the solid soil compartment (Jones and Glendinning 2006). The electro-osmotic process allows for the movement of another contaminant within the soil, which depends on the conductivity of soil and the pore water (Virkutyte et al. 2002). Electro-osmosis has been considered in soil consolidation due to its advantages in which the application of surcharge loads are not necessary and a significant reduction in the consolidation time being achieved (Wu et al. 2012). Due to the electro-osmotic consolidation of the soil, an improvement of about 100% to 200% in the soil shear strength can be observed (Lo et al. 2001). The effect of ionic diffusion in the soil allows for a permanent consolidation to occur after withdrawing the electrical supply with an additional increase in the soil strength (Lo et al. 2001). The soil strength at the anodes regions is greatly impacted (Staff 1998). From the EK experiments conducted by Eton (2011), a considerable increase in the force required to displace a pipeline is observed.

Micic et al. (2003) analyzed a three-dimensional (3-D) model with consideration of the material behaviours and boundary conditions. A two-dimensional (2-D) and 3-D numerical analyses are conducted by HU and WU (2014) based on the field test presented by Bjerrum et al (1967). A 2-D numerical study based on the field test reported by Bjerrum et al (1967) with consideration to the constitutive elasto-plastic behaviour and large strain of the soil is conducted by Yuan et al. (2015). Multi-Dimensional numerical analyses are presented by Yuan and Hicks (2015) with the field data being obtained from Burnotte et al. (2004). Numerical models with complex geometry, multiple electrodes, varying voltages and time of treatment were considered by Joshua and Kara (2018).

ELECTRO-OSMOTIC CONSOLIDATION OF SOIL

The principal effective stress σ' for a saturated soil is related to the pore water pressure u and the total stress σ given by the equation (Mitchell 1960):

$$\boldsymbol{\sigma' = \sigma - u} \tag{1}$$

The change in soil volume is controlled by the difference $\sigma - u$ (Mitchell 1960). Total pressure consist of various component within the soil and is considered to be the same at every points under equilibrium conditions. The flow of pore

water can occur within the soil if a difference is created at certain points. Component of the soil total pore pressure consist of osmotic and hydrostatic pressure (Mitchell 1960). Externally applied loads and partial saturation within the soil are main factors for the formation of the hydrostatic pressure while the potentials in the ionic concentration leads to the formation of the osmotic pressure (Mitchell and Soga 2005). The build-up of negative pore water pressure are mainly due to the electro-osmotic effect in saturated and partially saturated soil (Mitchell 1960).

Constitutive Equations

A mathematical model by Yuan and Hicks (2015) described the soil skeleton using Lagrangian coordinates and the porous liquid particle using the Eulerian coordinates with consideration to the configuration of the soil skeleton.

The water mass conservation is given as (Yuan and Hicks 2015):

$$\boldsymbol{\nabla}.(\boldsymbol{v^s} + \overline{\boldsymbol{v}}) = \mathbf{0} \tag{2}$$

Where v^s is the soil particle velocity and $\overline{v}$ is the water filtration velocity relative to the soil skeleton. The total flow due to the coupling of hydraulic and electrical gradient is shown in the equation below (Esrig 1968; Lewis and Humpheson 1973; Wan and Mitchell 1976):

$$\overline{\boldsymbol{v}} = -\frac{\boldsymbol{k_w}}{\boldsymbol{\gamma_w}}(\boldsymbol{\nabla p} + \boldsymbol{\gamma_w z}) - \boldsymbol{k_{eo}}\boldsymbol{\nabla \phi} \tag{3}$$

Where k_w is the hydraulic conductivity, γ_w is soil unit weight and z is the elevation, k_{eo} is the electro-osmotic permeability and ϕ is the electric potential.

The governing equation for the electrical field (assuming there is a conservation of electrical charge and steady state current) is given as (Yuan and Hicks 2015):

$$-\boldsymbol{\nabla}.\boldsymbol{j} = \boldsymbol{C_p}\frac{\boldsymbol{\partial \phi}}{\boldsymbol{\partial t}} \tag{4}$$

Where j is the electrical current flux, C_p is the electrical capacitance per unit volume. From ohms law and considering that the C_p is negligible, the electrical flow is given as

$$\boldsymbol{j} = -\boldsymbol{k_{\sigma e}}\boldsymbol{\nabla \phi} \tag{5}$$

Where $k_{\sigma e}$ is the electrical conductivity.

For a constant hydraulic pressure, the excess pore water pressure u_e is obtained from the equation (Esrig 1968; Lewis and Humpheson 1973; Wan and Mitchell 1976):

$$\nabla^2 u_e + \frac{k_{eo}}{k_w}\gamma_w \nabla^2 \phi = -\frac{1}{C_v}\frac{\partial u_e}{\partial t} \quad (6)$$

$$\text{And, } c_v = \frac{k_w}{m_v \gamma_w} \quad (7)$$

Where c_v is the coefficient of soil consolidation.

The high conductivity of subsea clay which requires a high power supply and the corrosion of the anodes are the two main challenges encountered with the EK process. These challenges can be lessened by applying electrical current on intermittent bases as stated by Lo et al. (2001). Voltage distribution between electrodes is approximately linear with no considerable drop. However, at the soil-water interface, a major decrease in the current flow can be observed due to a decrease in the soil conductivity (Lo et al. 1999). In this case, a polarity reversal can be used to achieve an increase in the current density (Micic et al. 2002, 2004; Wan and Mitchell 1976). The power consumption rate P is defined in Eqn.8 (Lo et al. 2001).

$$P = j \times \beta \times \Delta\emptyset/\Delta L \quad (8)$$

Where j is the current density, β is the intermittent power supply, $\emptyset$ is the applied voltage, and L is the distance between anodes and cathodes

Dynamic Pipe-Soil Interaction

Embedment of pipeline plays a vital role in controlling its displacement in axial and lateral directions. Many studies and designs were introduced to address this challenges. These ranges from understanding the behaviour of pipeline response to force and displacement, loading cycles, and point of failure (Cormie et al. 2009). Merifield et al. (2008) conducted a numerical analysis for the determination of pipeline embedment using wished in pipe (WIP) method where the pipeline is placed at a predefined depth and the pushed in pipe (PIP) methods where the pipeline penetration is due to its weight and operational loads as shown in Fig. 1 (Aubeny et al. 2005). The force to displace a PIP is greater than the WIP due to heave formation at the pipeline invert surface (Merifield et al. 2009).

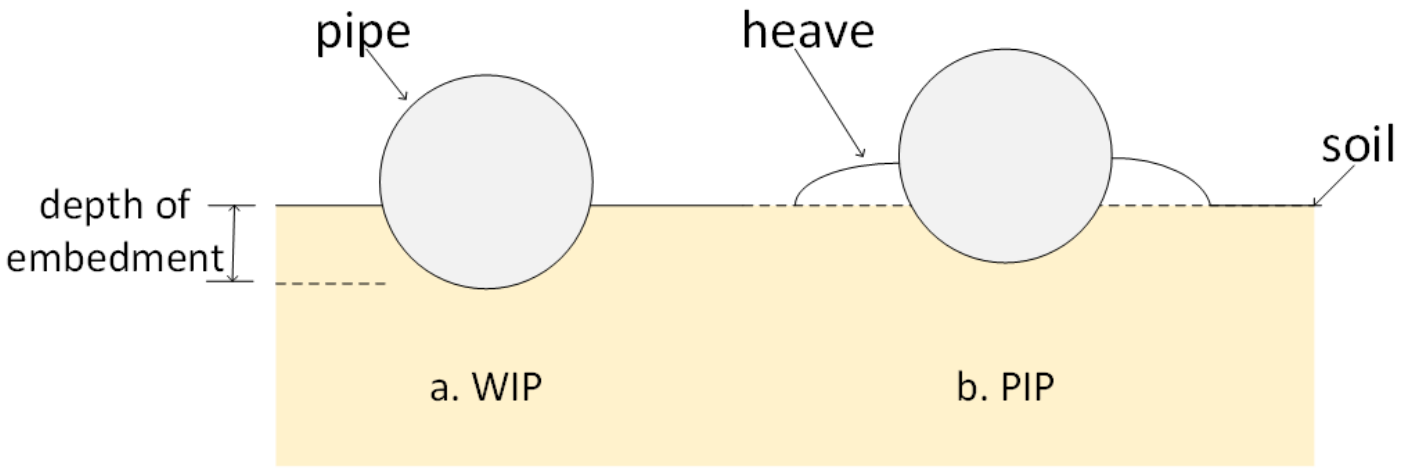

Fig. 1 a. Wished in Pipe, (WIP) b. Push in Pipe, (PIP)

The vertical reaction law defining the embedment of pipeline in the soil were explained in details by Muthukrishnan et al. (2011); Ballard and Falepin (2009); Randolph and White (2008); Westgate et al. (2010a), (2010b). The excess pore water pressure accounts for undrained or partially undrained conditions of the subsea pipe-soil interactions (Ballard et al. 2013). The drained and undrained state of the soil is determined from the relationship shown below (Randolph and House 2001).

The fully drained condition, $\frac{vD}{C_v} < \mathbf{1}$ (9)

The fully undrained condition, $\frac{vD}{C_v} > \mathbf{20}$ (10)

Where v is the pile velocity, D is the pile diameter and C_v is the consolidation coefficient of soil.

The design for axial displacement of the pipeline is considered in two stages which include the peak (breakout resistance) and residual resistance (Ballard et al. 2013; Bruton et al. 2008; Carneiro and Castelo 2011). The alpha approach can be used to determine the peak and residual resistance of a pipeline (Ballard and Falepin 2009; Casola et al. 2011; Oliphant and Maconochie 2006):

$$\boldsymbol{F = A_c S_u\, \alpha'} \quad (11)$$

Where, S_u is the soil shear strength, α' is the adhesion factor and A_c is the pipeline area of contact.

The axial effective force acting on the pipelines is governed by the equation (Ballard et al. 2013; Carr et al. 2008):

$$\boldsymbol{F_e = F_w + p_e\ A_e - p_i\ .A_i} \quad (12)$$

Where, F_e is the axial effective force, F_w is the axial force on pipe wall, p_e is the pipe external pressure, p_i is the pipe internal pressure, A_e & A_i are the pipe external and internal area respectively. For a condition at which the axial strain is zero, the axial effective force F_e of a fully constrained and closed ended pipeline is given by the equation (Ballard et al. 2013):

$$\boldsymbol{F_e = \frac{\Delta L}{L_0} EA + (1 - 2\upsilon')(p_e A_e - p_i A_i) - EA\alpha\Delta\theta} \quad (13)$$

Where, ΔL is the increment in length, L_0 is the original length, A is the steel pipe cross sectional area and E is the Young's modulus of elasticity, υ' is the Poisson ratio, α is the coefficient of thermal expansion and $\Delta\theta$ is the temperature gradient.

The lateral buckling design considered the break out force, the suction release, the residual force and the cyclic lateral force (Cormie et al. 2009). Many types of researches were conducted to find solutions to this problem which includes pipeline behaviour in response to the forces and displacement, cycles of loading and failure point (Cormie et al. 2009). Additional details are given by Altaee and Fellenius (1996); Bai and Bai (2014); Bruton et al. (2006), (2008).

This study uses the ABAQUS tool to determine the effect of EK on subsea pipe-soil interaction. Three stages are involved in the EK analyses: geostatic, electro-osmosis (consolidation), and dynamic analyses. The measurement and comparison of the resistance developed between the EK and non-EK treated soils are determined and compared.

MODEL DEVELOPMENT

The flowchart describing the EK analyses procedure is shown in Fig. 2. In the ABAQUS tool, the Geostatic procedure is first applied to ensure stress equilibrium within the soil and the soil procedure is adopted in the soil consolidation step. The last step considers the dynamic implicit procedure for the dynamic pipe-soil interactions which involves the EK and non-EK analyses. The analyses assumptions are: anodes and cathodes are made of same materials; the cathodes have zero electrical potential; the soil, water, and electrodes experience constant electrical conductivity; the fluid velocity is directly proportional to voltage gradient, and the pore pressure in the soil is uniform.

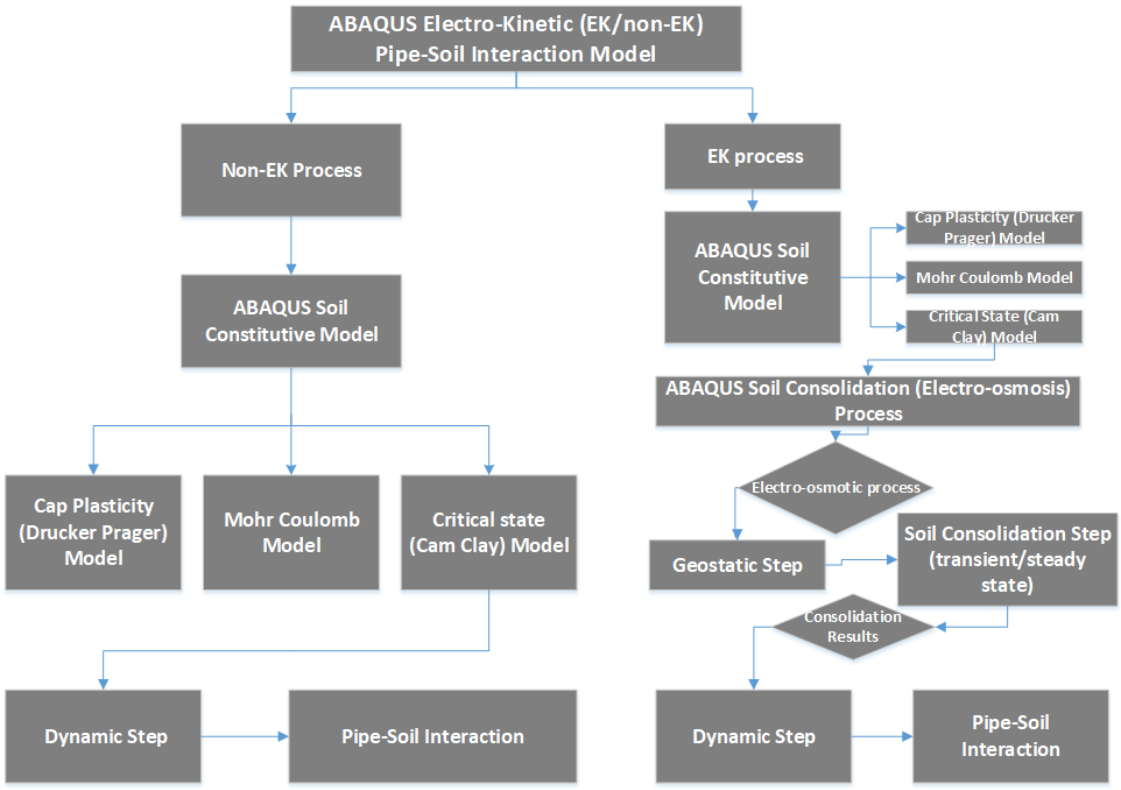

Fig. 2 Flowchart: ABAQUS EK/non-EK test process

Modelling Soil Electro-Osmotic Consolidation

ABAQUS tool does not have the direct capability to solve the electro-osmotic problems. However, a relationship has been established between the governing flow equations such as the electrical flow, heat transfer flow, fluid flow, and chemical flow (Mitchell and Soga 2005). Each of the flow processes can be used to mimic the other and in this case, the heat flow process to mimic electrical flows is adopted (Hansen and Saouma 1999; Mitchell and Soga 2005). In the ABAQUS tool, the heat flow process is based on Fourier law while the electrical flow process is based on Ohms law (Dassault Systèmes 2014). The procedure couple temperature-pore pressure element is used to model the electro-osmotic consolidation process. Tie interaction constraint is adapted to ensure electrical conductivity between the electrodes, soil, and water.

The temperature $\theta = \theta(x,t)$ is assigned to the electrodes to mimic the voltage $\phi = \phi(x,t)$. Pipe is unconstrained and assumed to be straight. The water level is set at the soil top surface where it is permeable with zero pore water pressure assumed. The soil surfaces is set to be permeable and displaces in the vertical direction while the soil bottom surface is set to be impermeable and fixed.

The analyses of the initial time increment are derived from Eqn. 14 as shown below (Ansari et al. 2014; Vermeer et al. 1981).

$$\Delta t_{initial} = \frac{h^2 \gamma_w}{6E'k} \tag{14}$$

Where h is the element average dimension, k is the permeability of the soil, and E is the effective Young's modulus. The parameter NLGEOM is set on to account for the geometry non-linearity during the analyses. The element sizes were determined using the convergence test. A 10-nodes modified quadrilateral tetrahedron, pore pressure and temperature, hourglass control, C3D10MPT is used to modelled the soil/water sections, support rings, and electrodes while a 6-node triangular thin shell element, STRI65 is used to modelled the pipe section (Dassault Systèmes 2014). The soil, electrode, pipe and rings have the element sizes of 0.0075m, 0.001m, 0.012m and 0.0008m respectively. The model consists of six anodes, two cathodes, and two supporting rings.

To establish the initial electrical contact between the anodes and the soil the WIP method is adopted as shown in Fig. 1. The pipe and electrodes assembly are described in Fig. 3 and the arrangement of the axial pipe-soil interaction are described in Fig. 4. The electrodes layout is further described in Fig. 5. The anodes and cathodes are inclined to the pipe at an angle of $20°$. The anodes are embedded in the soil while the cathodes are embedded in the water where the pore water drainage occurs. From Fig. 5, the approximate distance x between cathodes and anodes gives rise to the voltage gradient. The electrical flow can occur in all directions as the potential at the surface are assumed to be zero. However, as reported by Rittirong and Shang (2008), the electro-osmotic flow can be assumed to occur mainly in two dimensions of x-y plane provided that the distance x between cathodes and anodes is far lesser than the thickness U and width of the soil/water Z $(i.e\ U, Z \gg x)$.

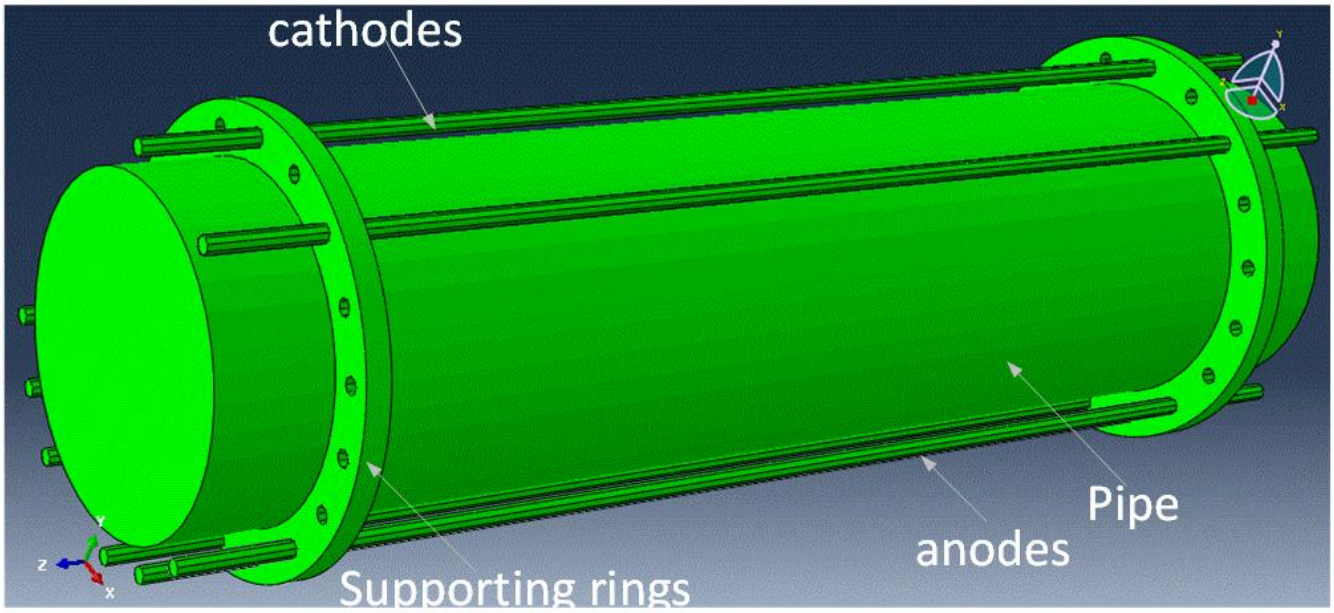

Fig. 3 Assembly of pipe, electrodes and supporting rings

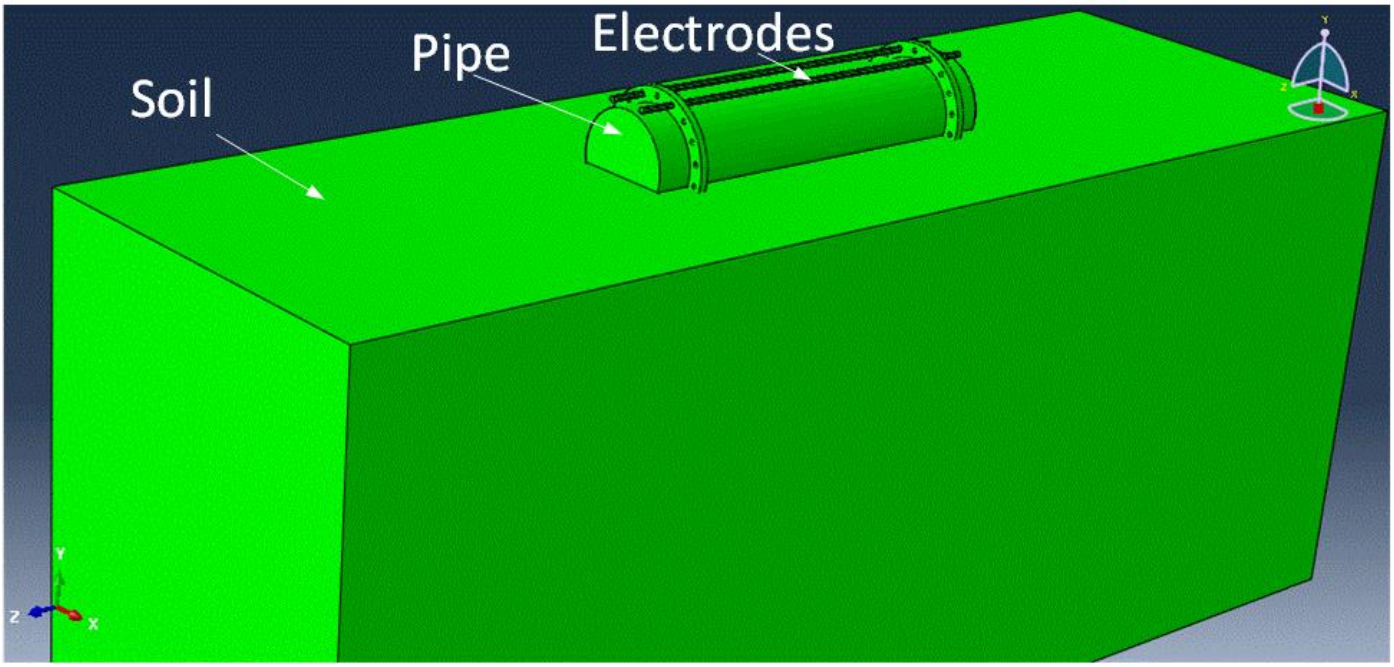

Fig. 4 Description of pipe-soil axial interaction model with the pipe partially embedded into soil

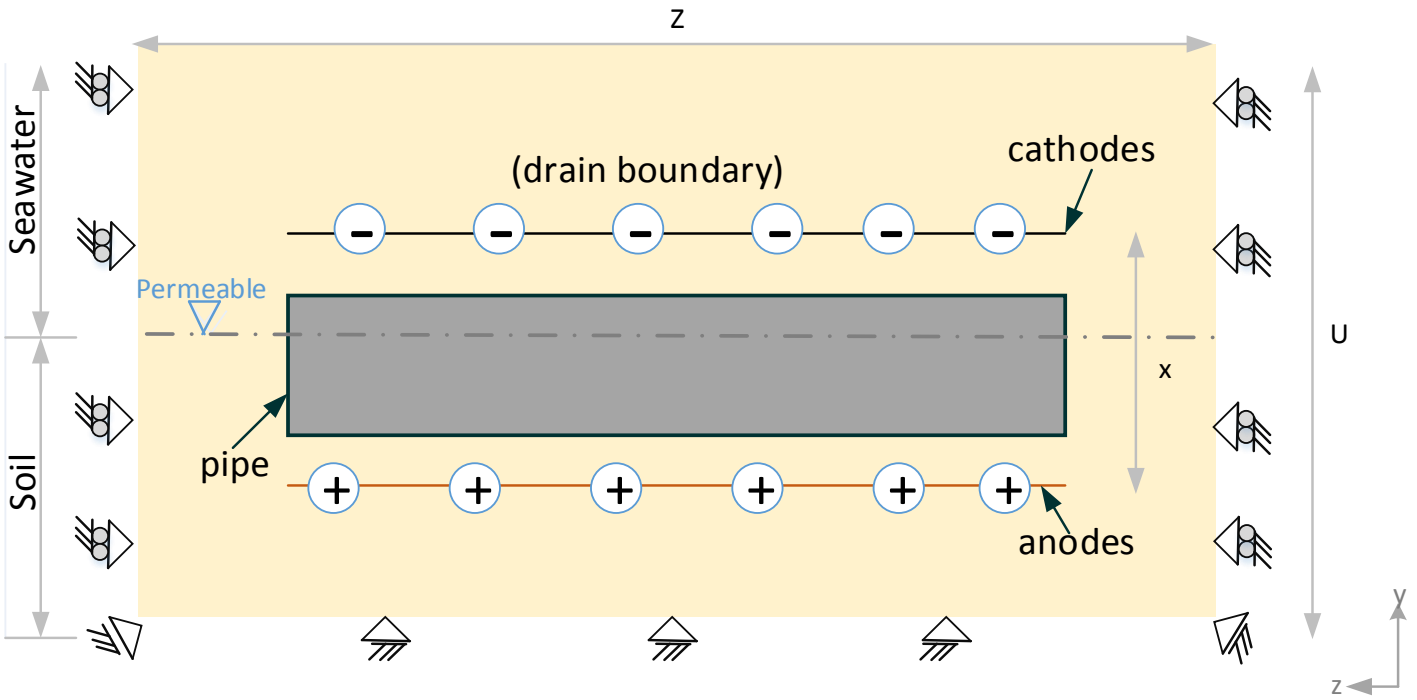

Fig. 5 The schematic model configuration of the electro-osmotic process.

Schematic arrangements of the model are described in Fig. 6, Fig. 7 and Fig. 8 represents the vertical penetration, axial displacement and lateral displacement of the pipe respectively.

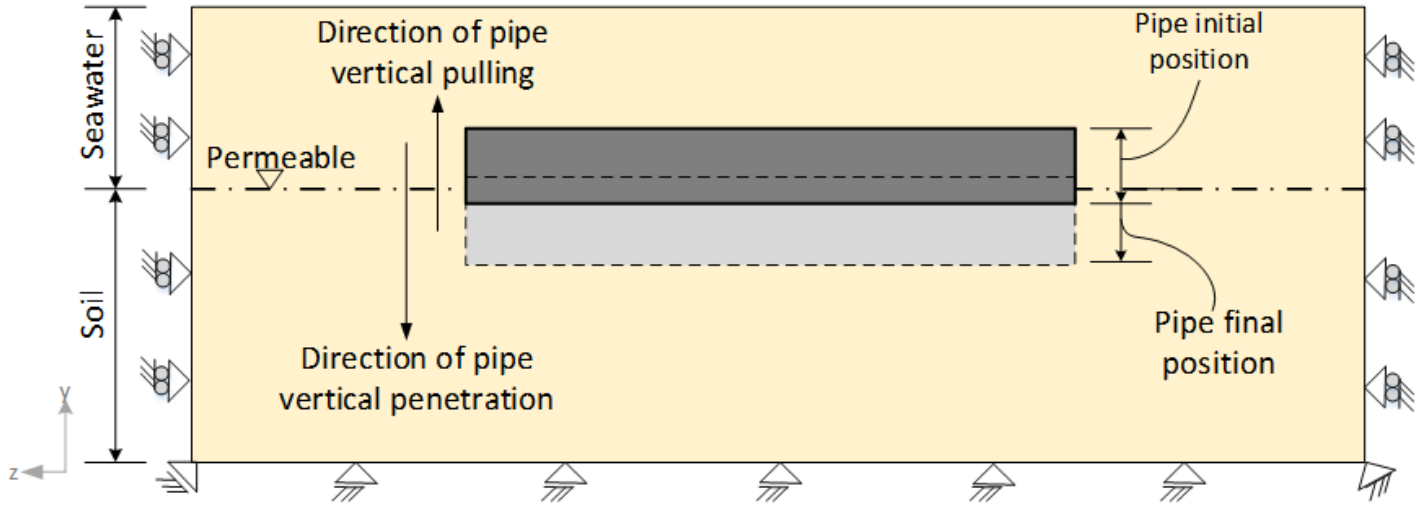

Fig. 6 Phase-2: Schematic Side view of model position for pipe vertical penetration test.

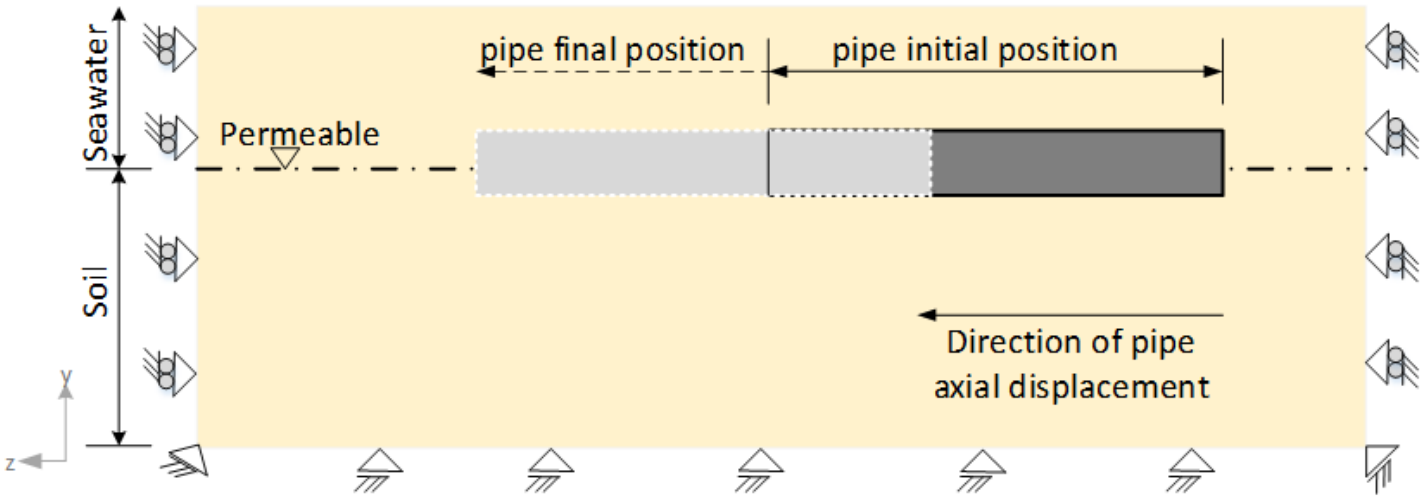

Fig. 7 Schematic of model position for pipe axial displacement test

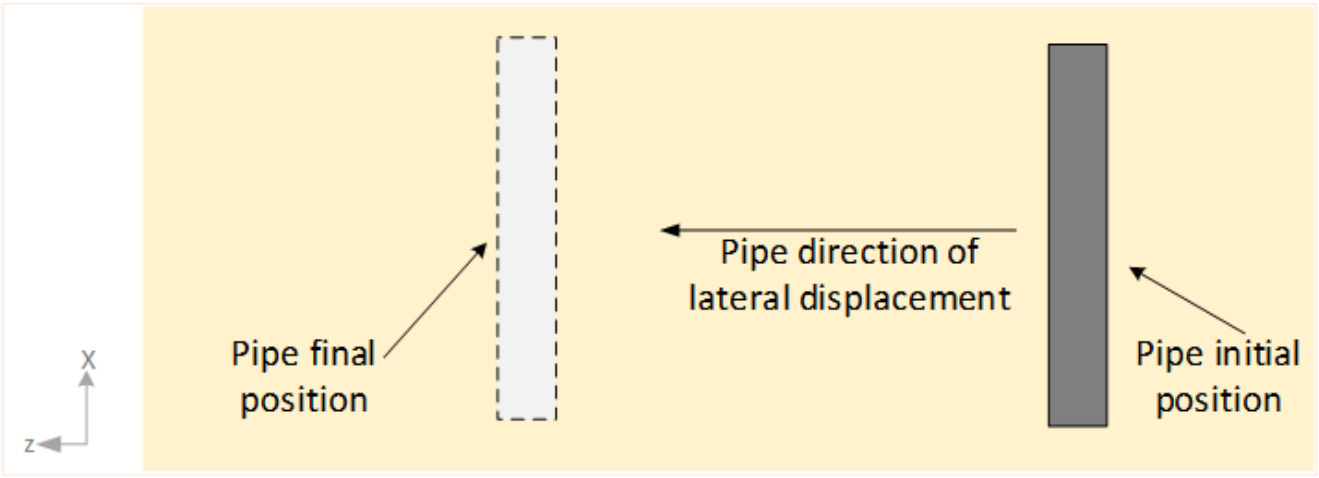

Fig. 8 Schematic Plan view of model positon for pipe lateral displacement test

Model Properties

The pipe is made of steel, the soil of kaolin clay the supporting rings of polypropylene materials. The iron material is considered for both the anodes and cathodes and as given by Eton (2011), The iron material is more effective for the electro-osmotic process in the soil-water medium when compared with copper and aluminium. Drainage normally occurs at the cathodes, however, due to the cathodes embedment in seawater, drainage occurs at the seawater surface. In this case, less number of cathodes are adopted as compared to the anodes. Due to the higher conductivity of seawater than clay soil, the seawater resistivity can be ignored (Eton 2011). The model and electro-osmotic properties are described in Table 1 and Table 2 respectively. The water has the depth of 0.055m and the soil has the depth of 0.105m. The data were

obtained based on small-scale modelling by Dutta et al. (2014), this was scaled by a multiplier factor of 40 to represent the large-scale experiment conducted by Dingle et al. (2008)**.**

Table 1 Pipe/Soil Model

Parameters		**Values**
Soil	length	0.258m
	width	0.084m
	depth	0.16m
Pipe	length	0.08m
	diameter	0.02m
Electrodes	length	0.08m
	diameter	0.001m
Supporting rings	outside diameter	0.026m
	inside diameter	0.02m
	thickness	0.0015m
	holes diameter	0.0012m
	angle between holes	20°

Table 2 Electro-osmotic/Cam Clay model parameters

PARAMETERS		MATERIALS	VALUES	UNITS
Electrical Conductivity $k_{\sigma e}$	(Callister and Rethwisch 2014; Engineering Toolbox 2015; Mitchell and Soga 2005)	Soil	1.0	S/m
		Seawater	4.8	S/m
		Iron electrode	1.0×10^{7}	S/m
Hydraulic conductivity k_w		Soil	$1x10^{-9}$	m/s
Electro-osmotic conductivity k_{eo}		Soil	$5.5x10^{-9}$	$m^2/V.s$
Saturation, S		Soil	120	%
Void ratio e_o		Soil	3	
Virgin consolidation line, λ	(Ansari et al. 2014)	Soil	0.4	
Recompression/swelling line k		Soil	0.115	
The slope of Critical state line M		Soil	1.8	
The coefficient of earth pressure at rest, k_o		Soil	0.8	
Wet yield surface size		Soil	1	
Poisson ratio ν		Soil	0.333	
Young Modulus E		Soil	$1.8x10^{6}$	MPa
Dry density γ		Soil	11.21	kN/m^3
Electrical potential (ϕ)	Anodes		10	V
	Cathodes		0	
Time (t)	Steady state			s

Dynamic Pipe-Soil Interaction

The dynamic pipe-soil interactions consider both the non-EK and EK analyses and results between the two are compared as described in Fig. 2. The model properties are given in Table 1 and Table 2 same as for the electro-osmotic process. The ABAQUS dynamic implicit procedure is adopted for the pipe-soil interaction analyses. To define the friction and slip of the pipeline on the soil, tangential behaviour with a rough coefficient of friction and hard contact for the normal behaviour is set as given in the ABAQUS tool. The surface to surface interaction used to model contact between two surfaces

moving relative to each other is adopted with the soil and pipeline being the slave and master surface respectively. Displacement of the soil is allowed in the vertical direction of the soil surface and no displacement at the bottom surface is permitted.

Detail analyses with regards to vertical penetration of pipeline have been discussed by (Dingle et al. 2008; Dutta et al. 2014). However, the dynamic analysis investigates further the EK effect on the pipe under the same and also different conditions for a non-EK treated soil and EK treated soil. During vertical displacement analysis, the pipeline is penetrated further from the initial depth of 0.375D to a depth of 0.825D. The axial and lateral displacement analyses also undergo the same treatment as for the vertical displacement analysis with regard to the initial embedment. The vertical velocity of 0.015D and axial/lateral velocity of 0.0002m/s are applied to pull the pipeline. These velocities are adequate to give rise to an undrained condition in the soil as shown in Eqn. 10.

ASSESSMENT OF ELECTRO-OSMOTIC CONSOLIDATION

Electrical field distribution within the soil is shown in Fig. 9 and Fig. 10. The nodal temperature (NT11) as given in Fig. 9, mimic the voltage flow (V). From Fig. 11, the flow can be seen to concentrate more at the anodes region and gradually dissipate toward the cathodes region. At point 0.52m, the concentration of 10V decreases to 9V and with the further flow, this tends to zero at point 2.2m. However, at this point of 2.2m, the voltage is noticed to increase to 1.6V, due to embedment of cathodes inside the seawater where the pore water drainage takes place. From Fig. 11, the distance between anodes and cathodes set up the voltage gradient which gives the driving force for the pore water flow within the soil and the water medium, and as stated earlier, the seawater resistivity can be ignored due to higher conductivity of seawater than the clay soil. For optimum performance in service, one of the following options may be explored: by reducing the distance between anodes and cathodes, by increasing the voltage or by increasing the EK treatment time.

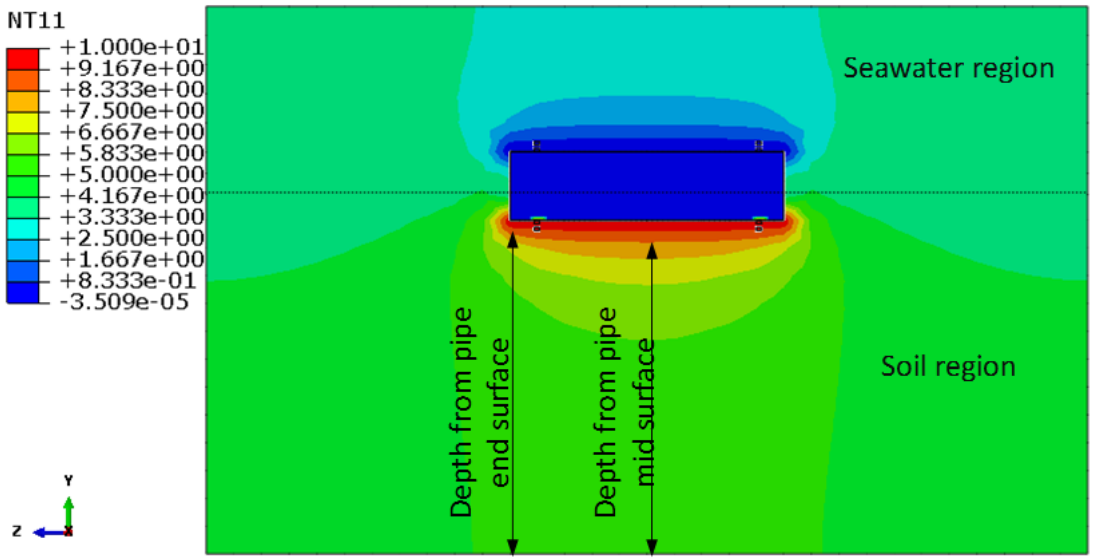

Fig. 9 A front section view of electrical field distribution within the soil and water regions

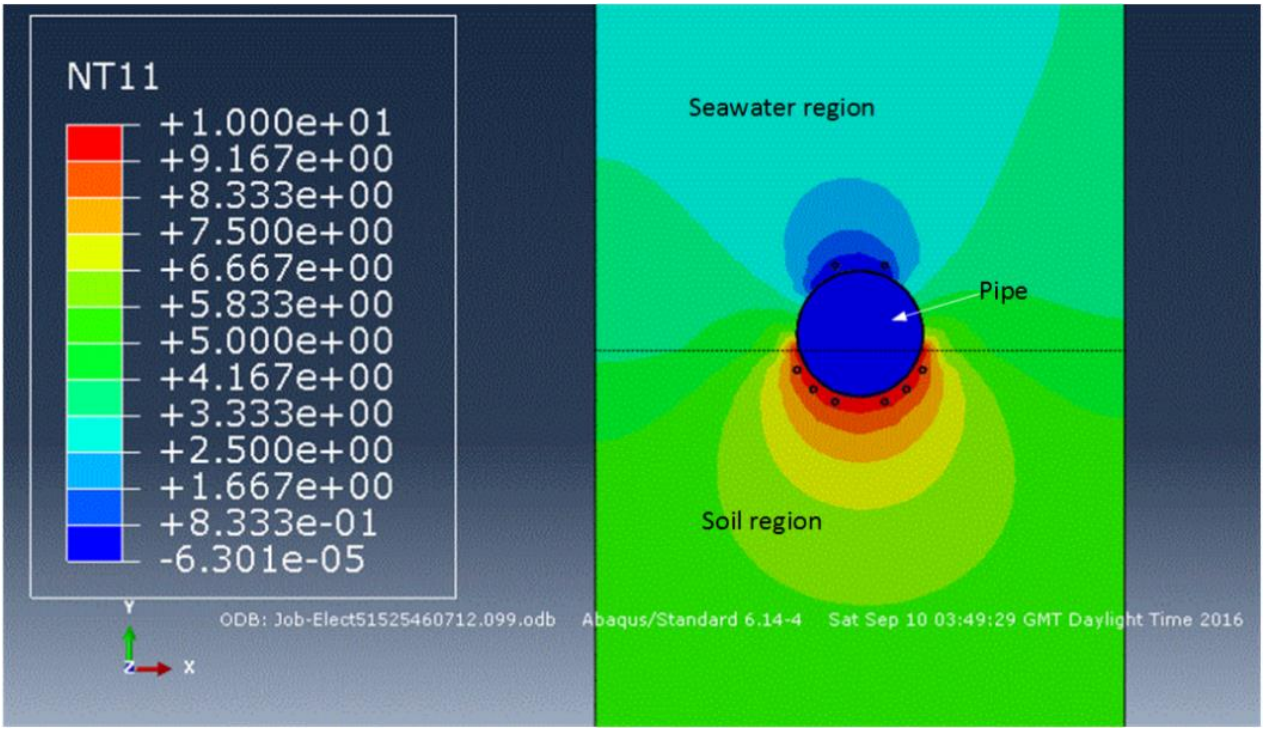

Fig. 10 A side section view of electrical field distribution within the soil and water regions

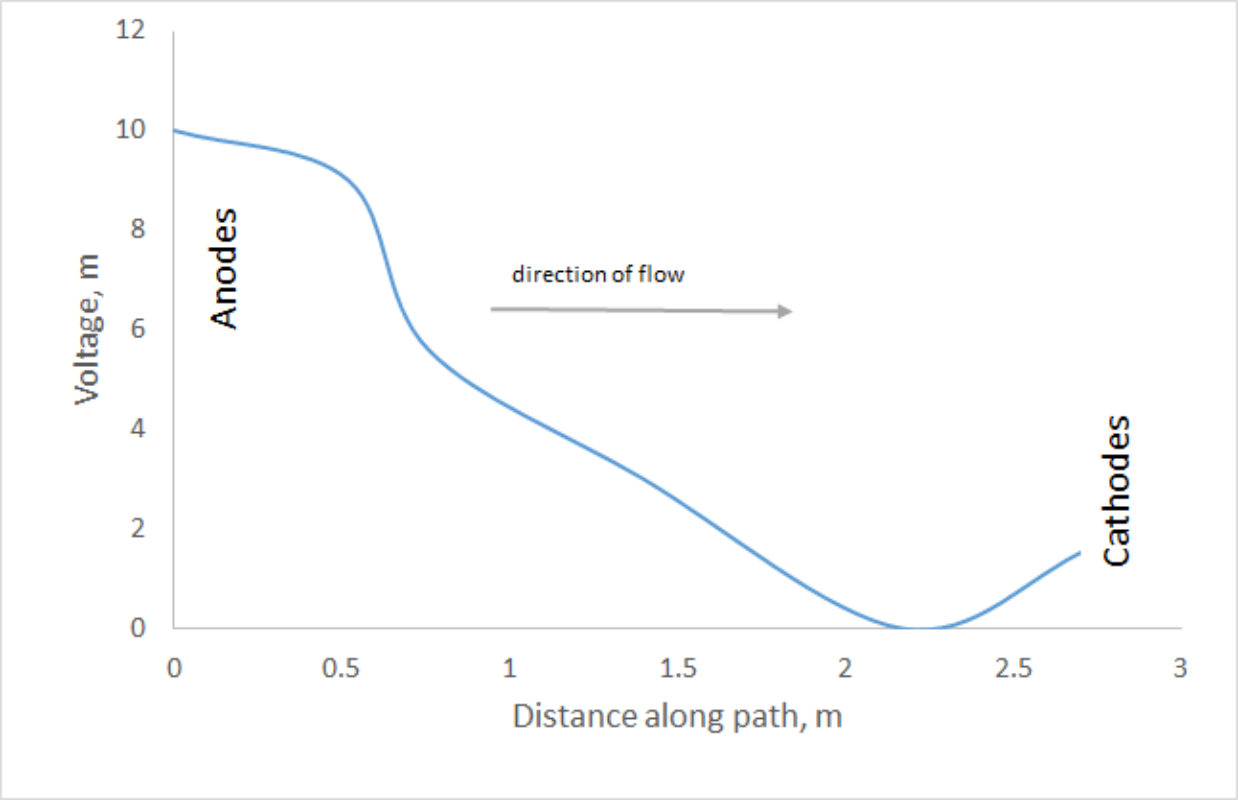

Fig. 11 Electrical field distribution during the electro-osmotic flow process

EK Area of Influence

Areas of influence of the model are shown in Fig. 9 and Fig. 10. The flow is also noticed towards soil horizontal surfaces and with depth as shown in Fig. 12. As earlier stated, the flow towards other surfaces is due to zero potential assumed. The EK influenced extended to a 4.1m depth from the pipe bottom surface. The area of influence at the end surface of the pipe is less than from the bottom mid-surface of the pipe. The flow concentration indicates a decrease with depth further away from the anodes. The midpoint of the pipe decrease in flow concentration to less than 5.2V while the pipe end surface decreases to 5.0V, accounting for a voltage difference of 0.2V.

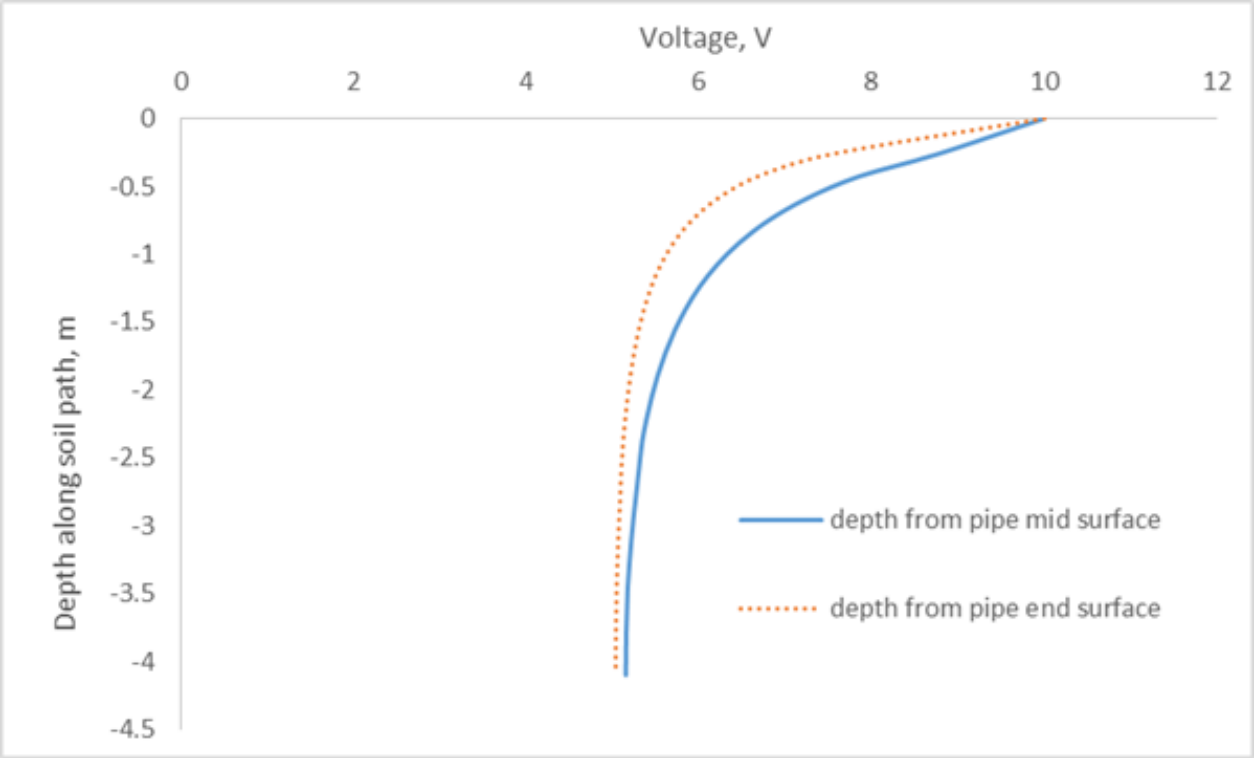

Fig. 12 Area influence by electrical field flow from pipe invert surface

Pore Water Pressure Dissipation

The voltage gradient of 4.55V/m gives rise to the pore water dissipation from the soil. The pore water pressure in the soil shows a gradual reduction and tend to negative near the anodes regions as it drained towards the cathodes as shown in Fig. 13. The dissipation of pore water pressure led to the gradual decrease in soil void ratio from its initial state of 3 to 1.554 as shown in Fig. 14. The largest decrease in the void ratio is experienced near the pipe surface due to its closeness to the EK region with a higher concentration of the electrical field. As shown in Fig. 15, the pore water pressure indicates a relatively constant state to a depth of 0.52m at a void ratio of 1.743. This depth effectively accounted for the soil settlement.

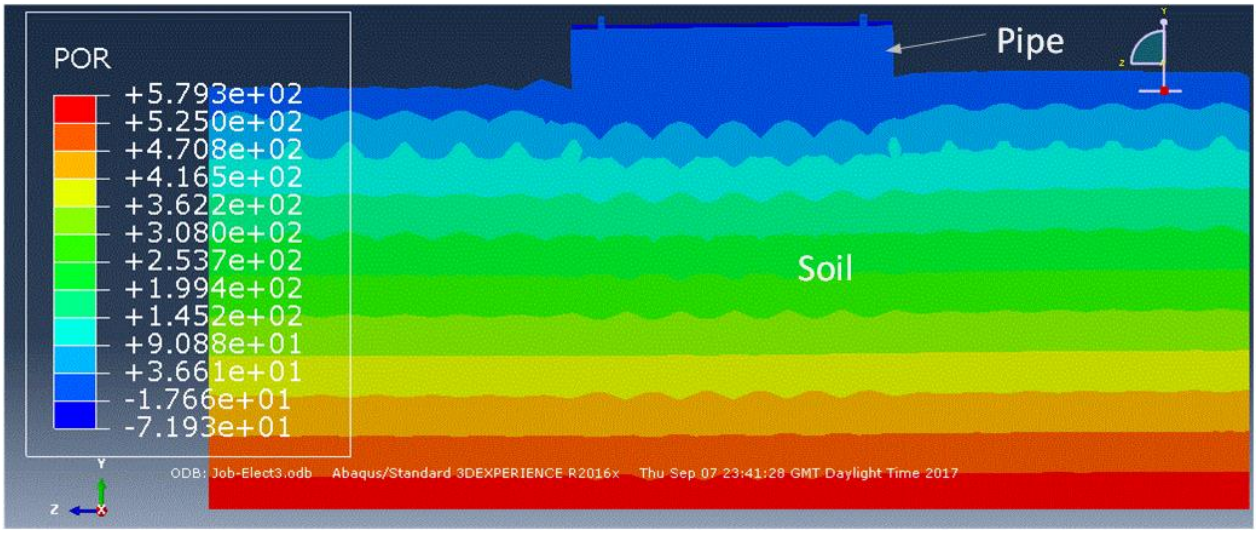

Fig. 13 Contour plot showing a cross section of the soil pore pressure distribution with depth due to EK effect

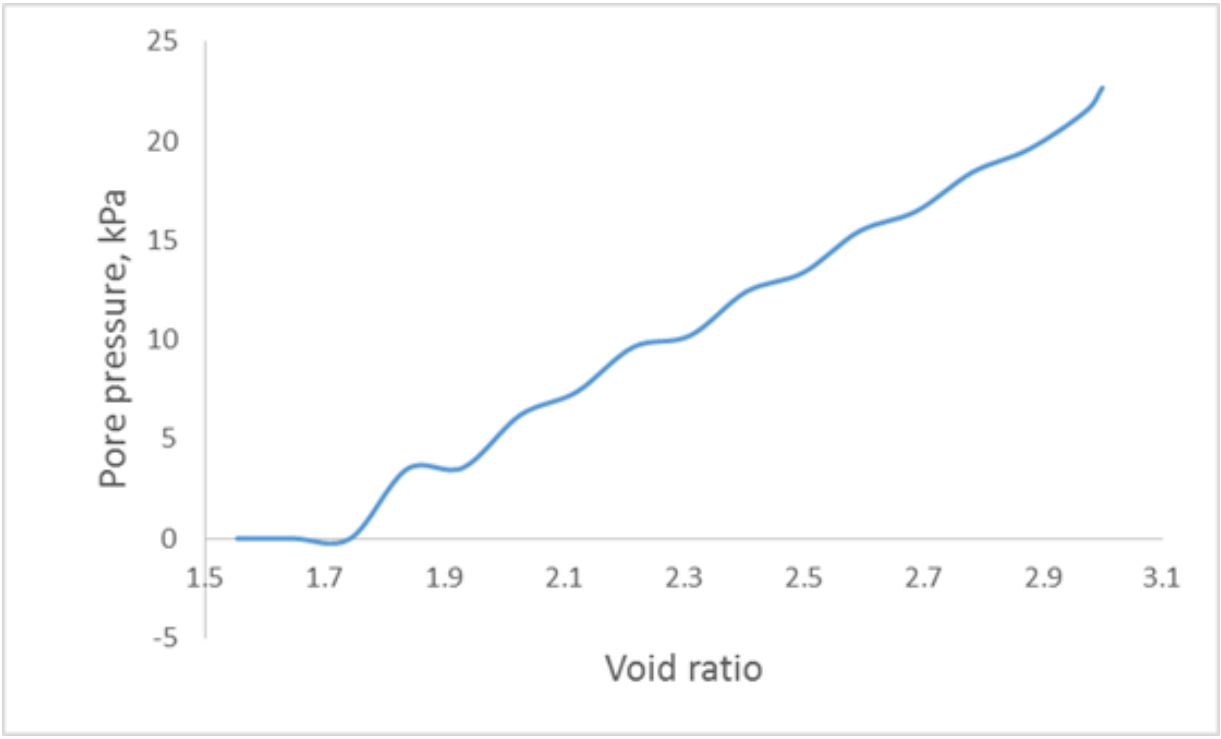

Fig. 14 Effect of the variation of pore water pressure dissipation on void ratio across soil depth.

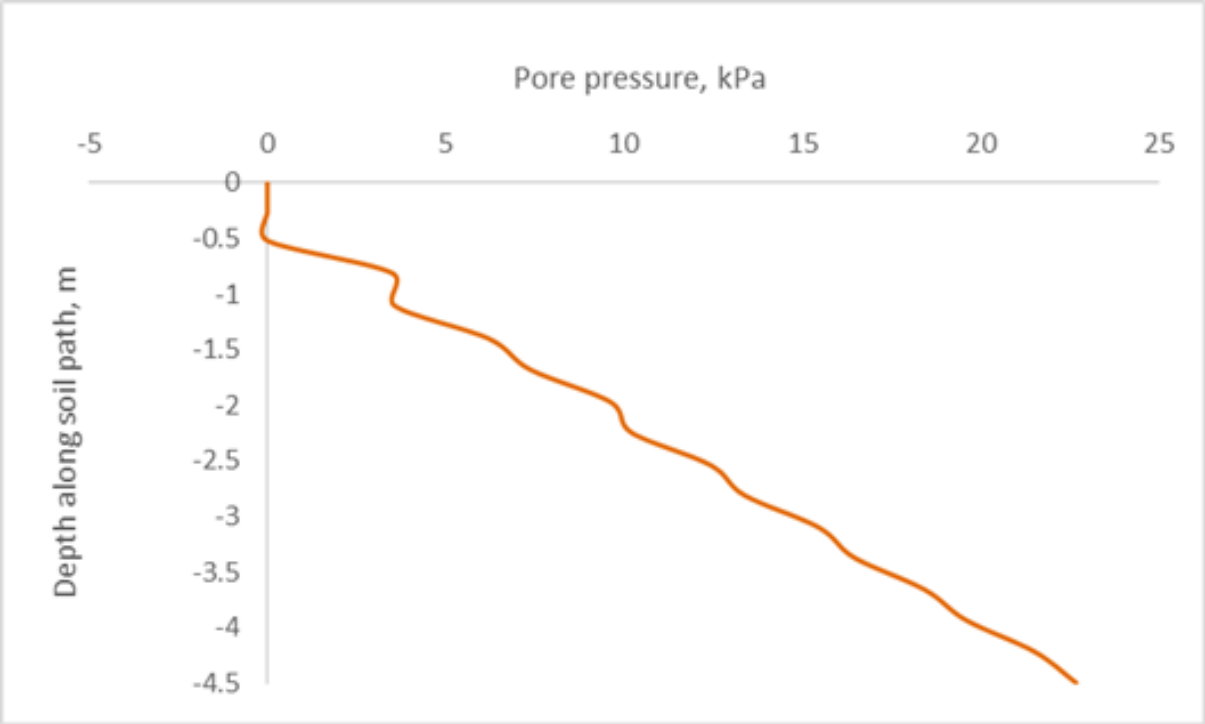

Fig. 15 Pore water pressure distribution within the soil

Effective Stress

The effective stress distribution within the soil is shown in Fig. 16. The effective stress experiences an increase as it approaches the soil surface. This behaviour occurs from the soil depth of 0.8m close to the anodes as shown in Fig. 16. This stress accounts for the increase in the force required to displace a pipeline from its initial position.

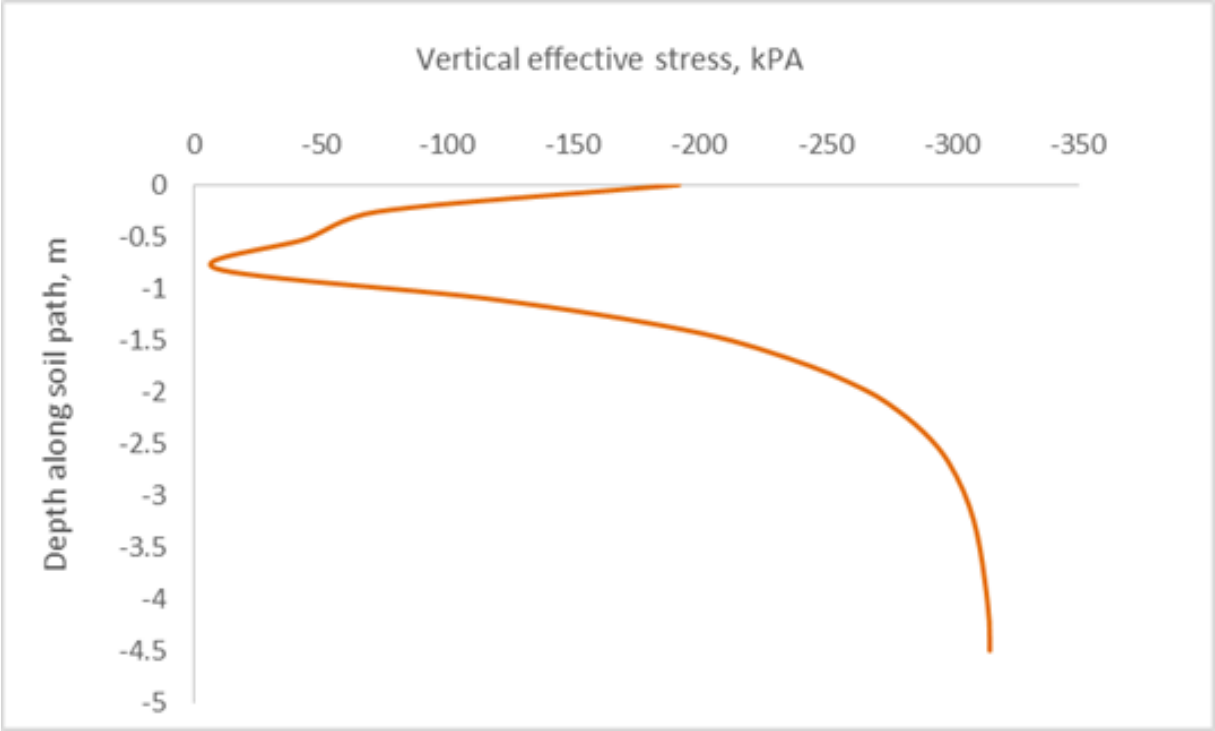

Fig. 16 Effective stress distribution along soil path

Soil Settlement

The contour plot of soil settlement is shown in Fig. 17. Maximum soil settlement of 2.09mm has been achieved for the EK process. The non-EK results are based on data obtained from small-scale modelling by Dutta et al. (2014) and when scaled by a multiplier factor of 40, this represents the large-scale experiment by Dingle et al. (2008). In this case, a soil settlement of 83.6mm is achieved for the EK process when compared with the 17.63mm obtained from the non-EK process as shown in Fig. 18. This account for a settlement of 3.8% when compared with the average distance between anodes and cathodes of 2.2m. Further effects due to the EK soil consolidation are given in the dynamic analyses section.

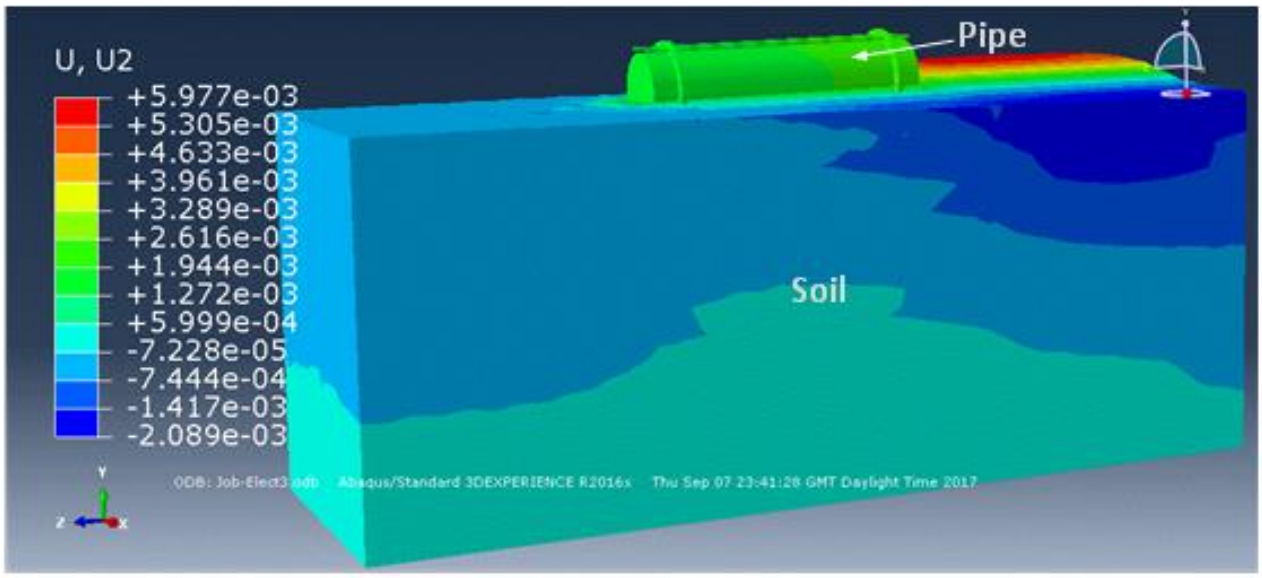

Fig. 17 Contour plot of soil settlement due to EK effect

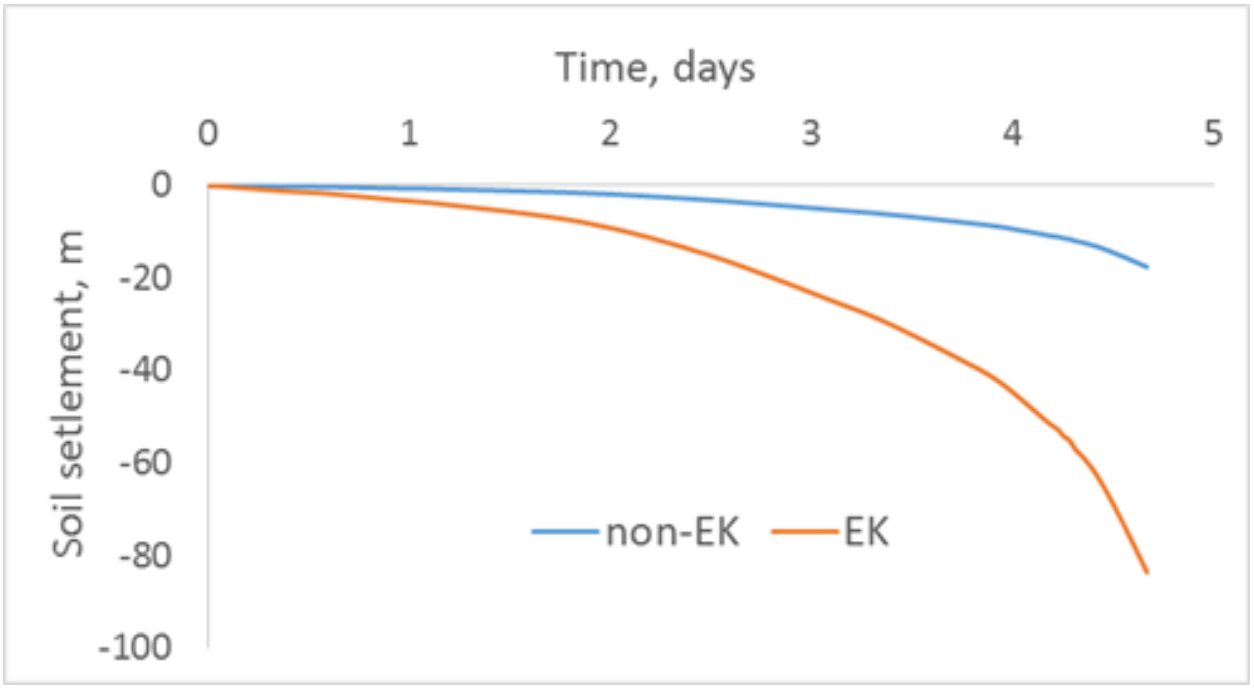

Fig. 18 Vertical soil settlement distribution within the soil due to non-EK and EK process

ASSESSMENT OF DYNAMIC PIPE-SOIL INTERACTION

Results from the dynamic pipe-soil interactions are presented for a pipeline under vertical, axial and lateral displacements. Both non-EK and EK analyses were conducted and result from each compared to determine their effect.

Effect on Pipe Vertical Penetration

The force-displacement reaction of the pipeline due to vertical penetration is shown in Fig. 19. Results from the non-EK treated soil are compared with a non-EK experiment conducted by Dingle et al. (2008) and non-EK numerical analysis conducted by Dutta et al. (2014). The penetration force shows a gradual increase with depth for all the processes. The EK process shows higher penetration force than the non-EK: approximately 95% increase is achieved.

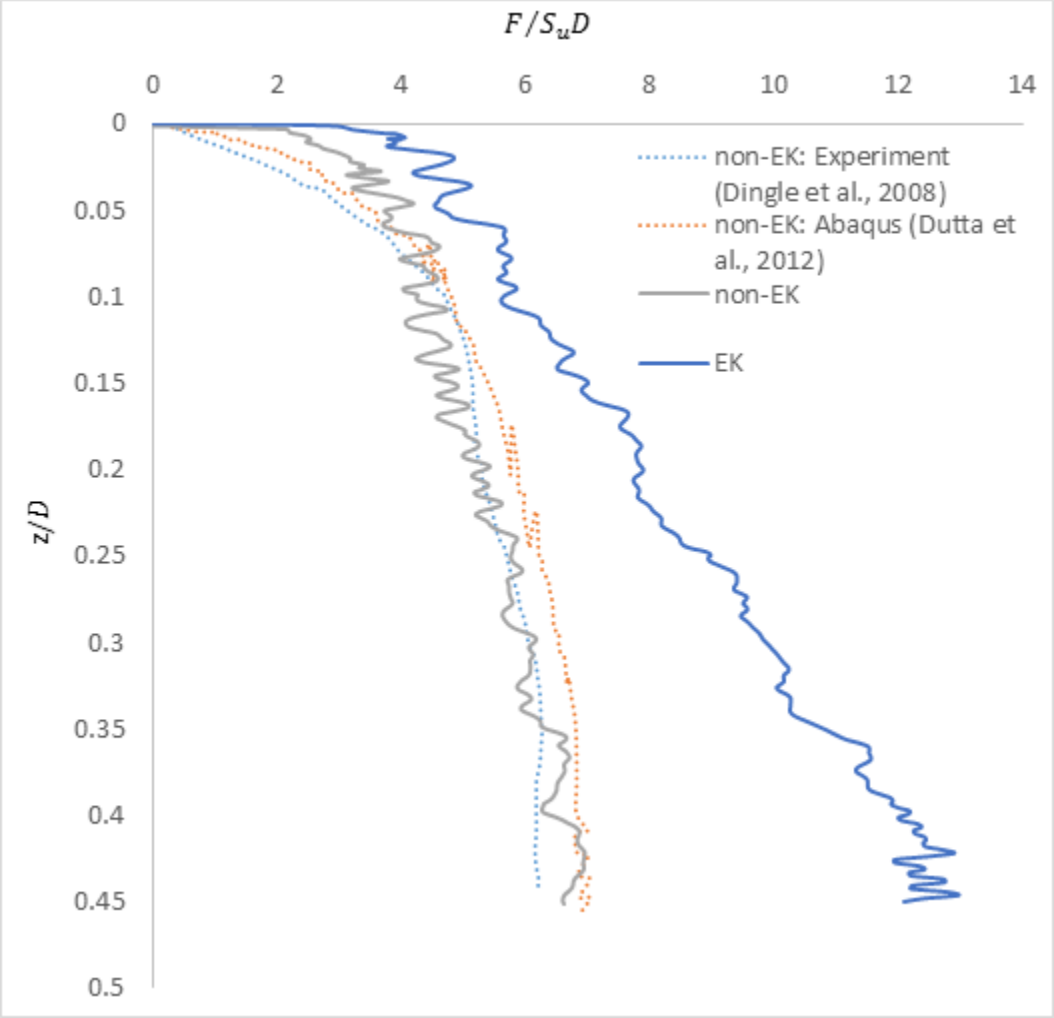

Fig. 19 Forces developed due to pipe vertical penetration

Effect on Pipe Axial Displacement

The pipeline is subjected to axial pulling as shown in Fig. 20. Pipe displacement behaviour on non-EK treated soil shows a peak force of 5N at a distance of 0.06m. On further displacement of the pipe, the peak force slightly decayed to a residual force of 4.4N. This residual force maintained approximately steady state to a distance of 0.52m before it

gradually increases. The EK treated soil experiences a peak force of 12.9N, which breaks at 0.055m. Further displacement of the pipe shows a gradual increase in the residual force. This behaviour is attributed to the soil conditions and the regions that are influenced by the soil treatment.

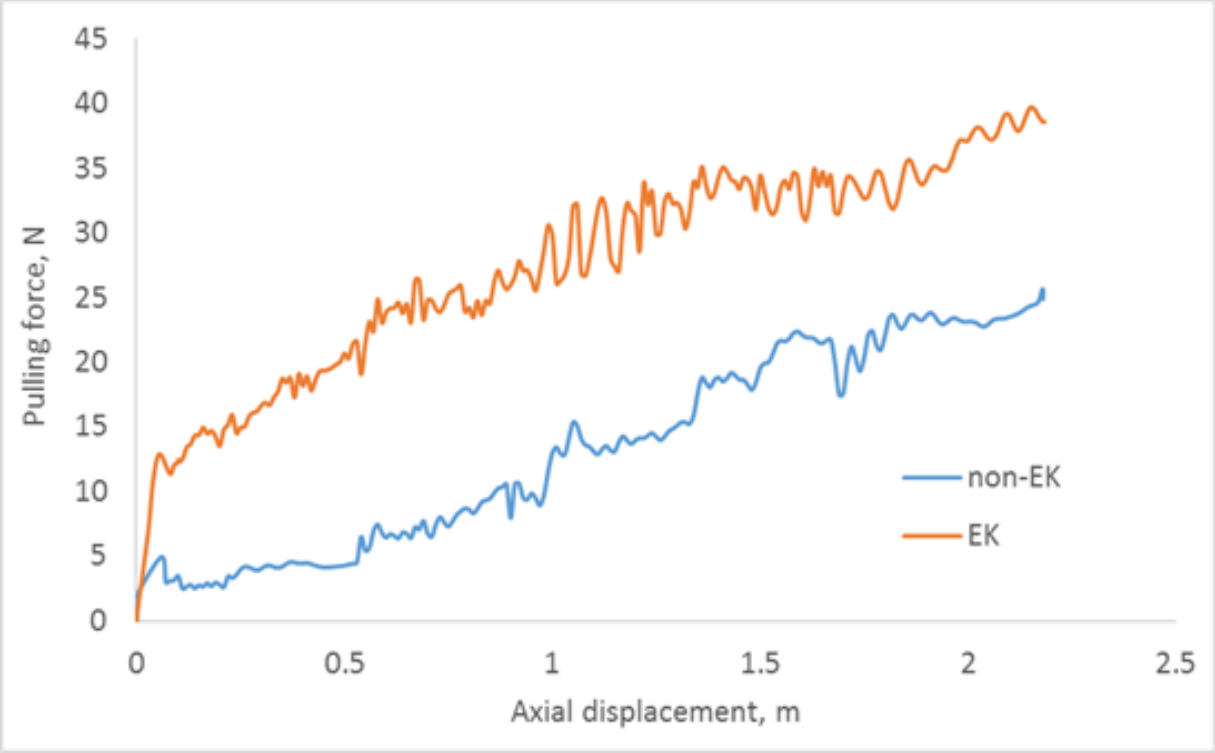

Fig. 20 Forces developed due to pipe axial displacement

A comparison of axial displacement of the pipe between the EK and non-EK treated soil as shown in Fig. 20 a 158% increase in the breakout force is achieved. As stated by Lo et al. (2001), a normally consolidated soft clay have shown to be over-consolidated when treated and the over-consolidated ratio can be achieved in the range of about 1.2 and 1.7 while the soil shear strength can witness an increase of about 100% to 200%. A comparison of the percentage increase in soil strength with a more recent electro-osmotic soil modification experiment by Eton, (2011) as shown in Fig. 21, an increase in the peak pulling force of 158% is observed. These increase in the axial pulling force due to EK effect indicates an improvement in the soil strength by over 100%.

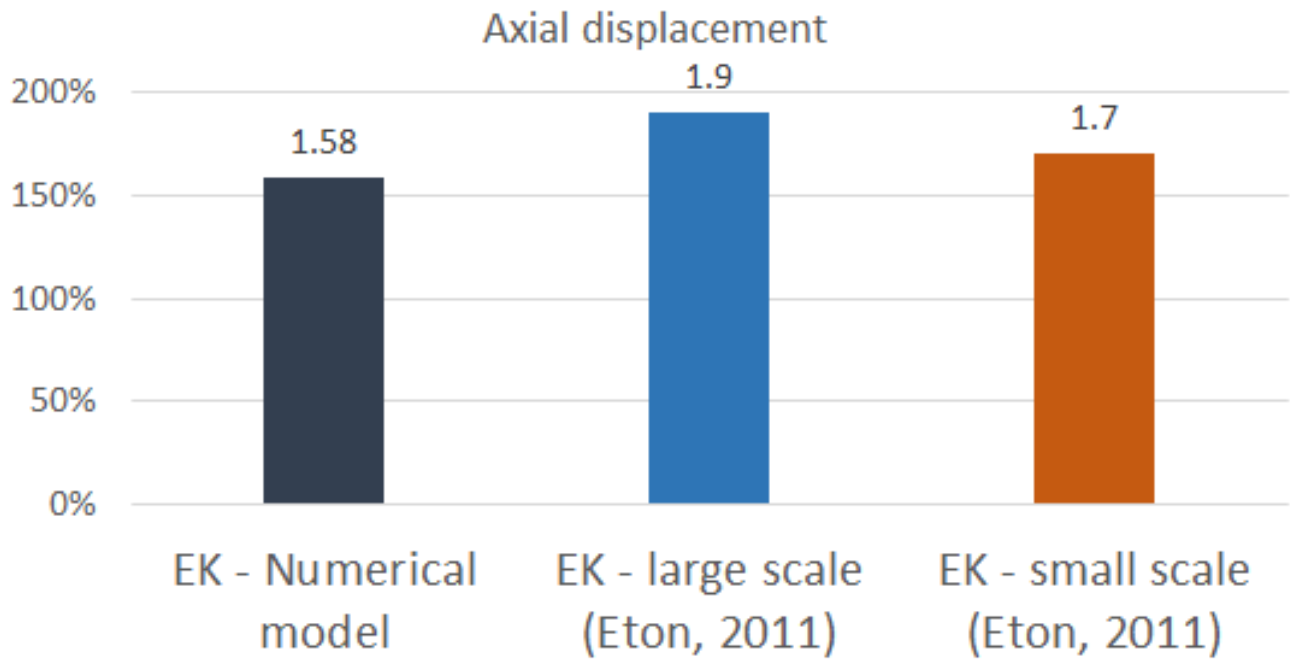

Fig. 21 Comparison of percentage increase on axial breakout force due to EK effect

Effect on Pipe Lateral Displacement

Results from the lateral pulling test are shown in Fig. 22. The peak force for the non-EK treated soil is 4.5N indicating higher stiffness, which breaks at 0.006m. The EK treated soil also shows higher stiffness tangent with the peak force of 11.5N which break at 0.1m. As the break out force is achieved, the residual force for both the EK and non-EK maintained a steady increase.

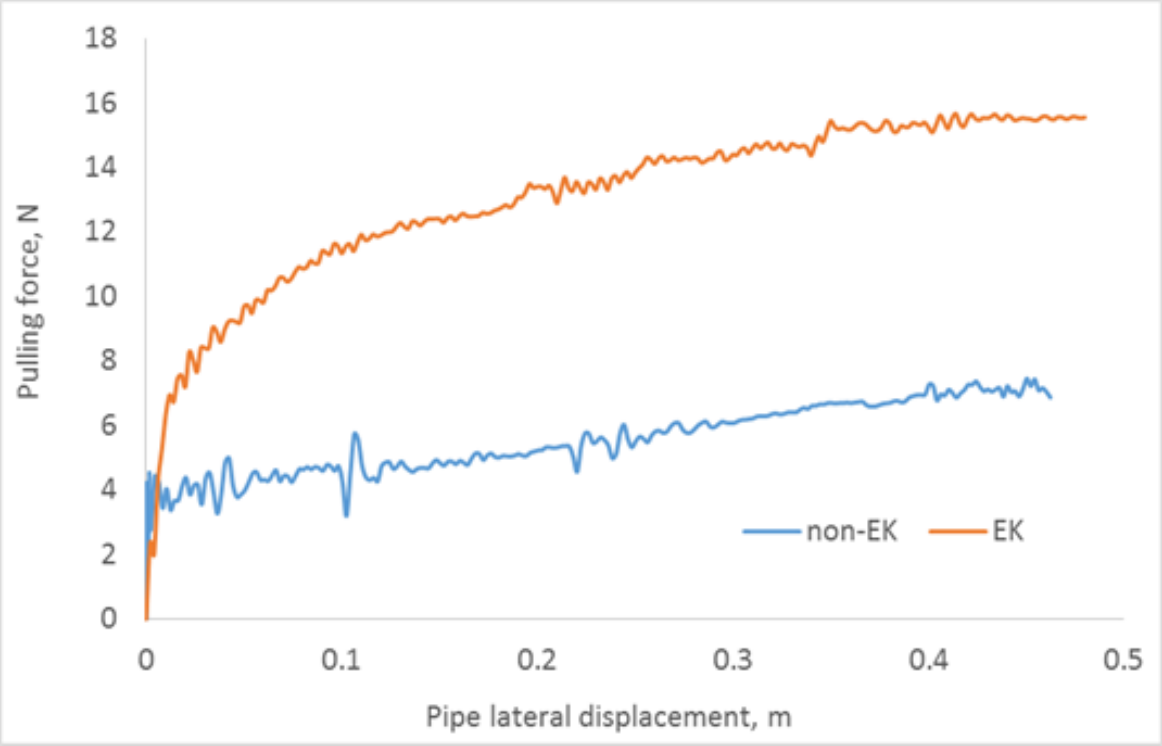

Fig. 22 Force s developed due to pipe lateral displacement.

Comparing the EK with non-EK treated soil as shown in Fig. 22, the lateral peak force due to EK effect indicates over 156% increase. From Fig. 23, the lateral peak force show a higher improvement than the experiment conducted by Eton, (2011).

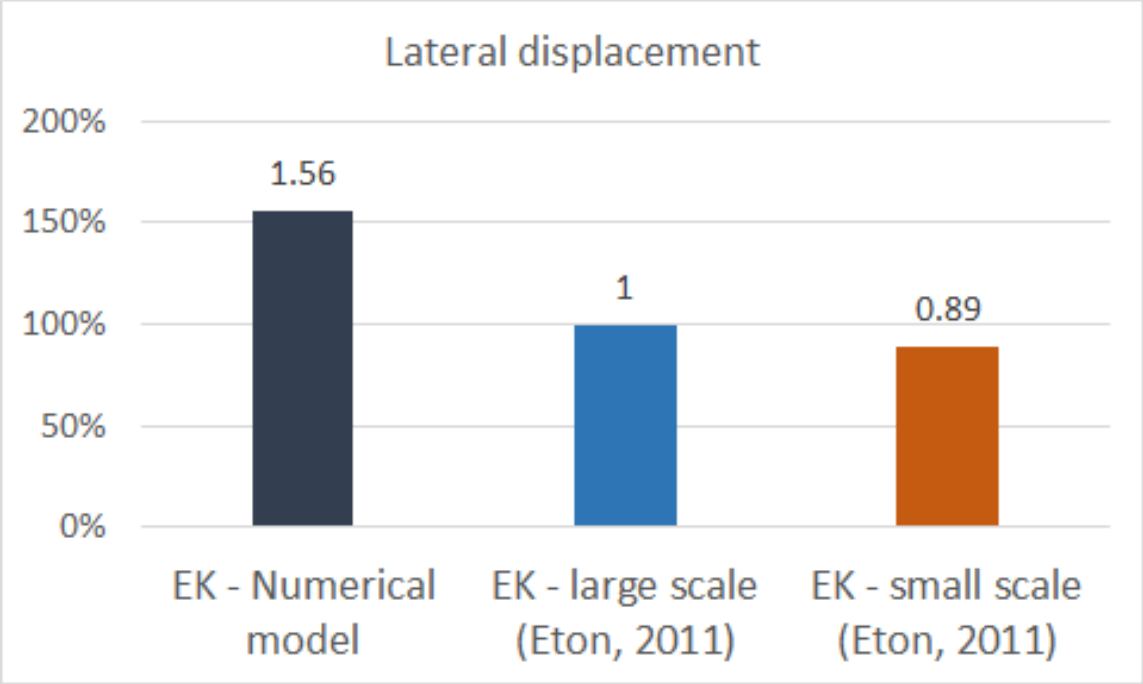

Fig. 23 Comparison of percentage increase on lateral breakout force due to EK effect.

Field Application

It has been established by researchers that increasing the soil strength is a possible mitigation approach. This new concept is introduced to serve as a mitigating measure against pipeline displacement and may be incorporated into a new subsea pipeline design or preinstalled at predetermined positions with regards to the cost and operating conditions. The subsea umbilical cables may be used as a power supply source. This concept will also find applications on underwater cables.

Snake lay method of the subsea pipeline is shown in Fig. 24 (Perinet and Simon 2011). The methods reduce the axial displacement of the pipeline with some limitations posed by the uncertainty in controlling lateral buckling (Rong et al. 2009). The anchoring points have been suggested by Eton (2011) as described in Fig. 24. Ideally, pipeline displacement at this point is not permitted hence, the EK process may be applied. Axial displacement occurs mainly on the short pipeline with a length usually between 2-5km (Bruton et al. 2008). One disadvantage of operating in the saline environment is the high rate of power consumption, however, a small volume of soil consolidation is required to increase the resistance to pipeline displacement as stated by Eton (2011). In this case, less power supply will be involved. Assessment of the soil properties and the pipeline embedment during installation and in operating condition will help to determine the electrodes configuration and power requirement for each individual case.

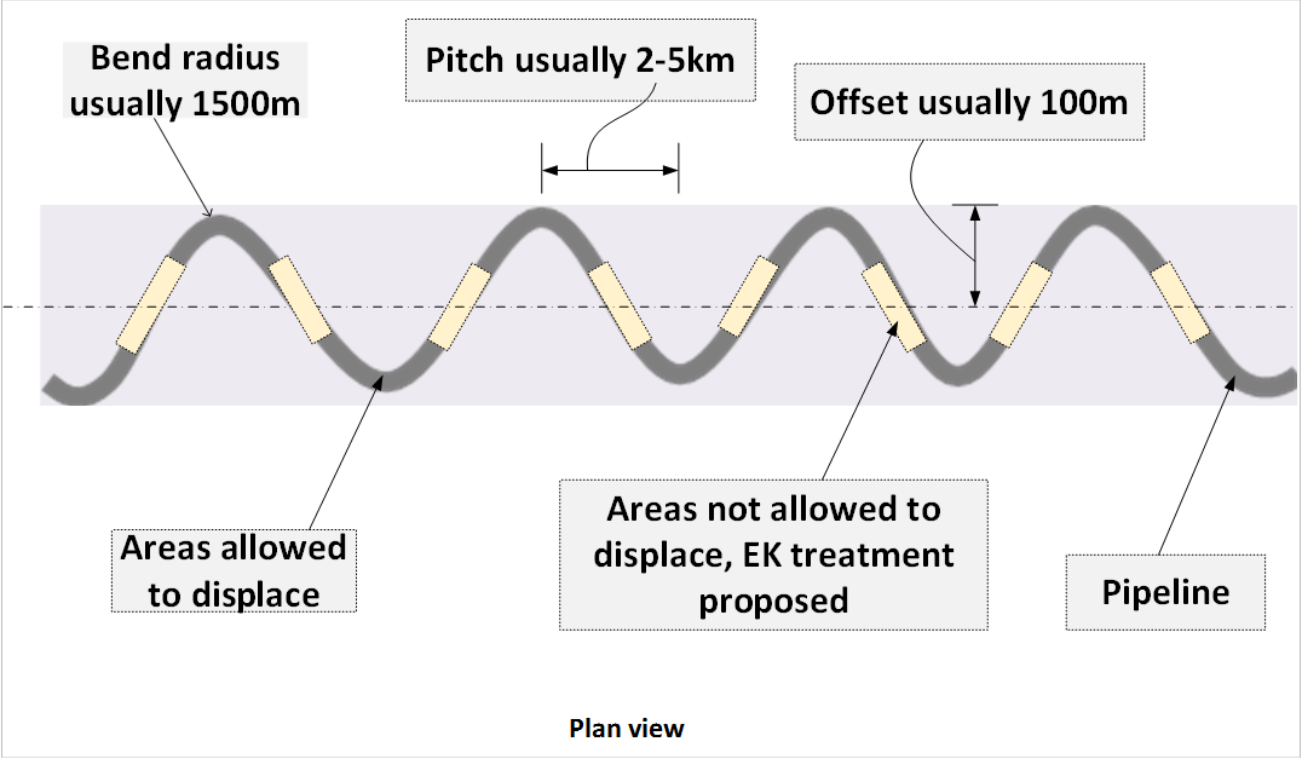

Fig. 24 Snake lay method of pipeline showing positions for EK treatment.

CONCLUSION

The EK effect on subsea pipe-soil interactions has been determined. The developed model shows the electrical field behaviour and the influence on pipe displacement. Electro-osmotic consolidation of the soil is mainly due to the dissipation of pore water pressure and a decrease in the soil void with a corresponding increase in the soil effective stress. The process was greatly influenced by the applied voltage which induces the pore water flow. The resultant effect of the electro-osmotic consolidation on dynamic pipe-soil interaction on both non-EK and EK under the same conditions were considered and results compared. Major areas in the dynamic analyses are the peak and residual forces generated due to the soil treatment. The resultant effect of pipe displacement in vertical, axial and lateral direction was also demonstrated. Comparing the EK over non-EK, the force required to displace pipeline shows a significant increase. A 95% increase in the vertical penetration force, a 158% increase in the axial pulling force and a 156% increase in the lateral pulling for the pipeline are observed. Due to the effectiveness of the EK method as indicated in the obtained results, this approach can be included in a new design of subsea pipelines or underwater cables and can also serve as a benchmark for further studies.

Further Studies

- Transient analyses with varying voltages to determine the sensitivity to this effect.
- Effect of Polarity reversal to enhanced on the EK treatment
- Assessment of electrochemical reactions with consideration to the insulation of pipeline and inline structures from interfering with the EK process.
- Pipe displacement with consideration to different velocities and loading conditions.

Acknowledgements

Appreciation to the Petroleum Technology Development Fund (PTDF) Nigeria for funding and support provided.

Notations

A	Surface area (m^2)
A_c	Area of contact (m^2)
C_p	Electrical capacitance per unit volume (F/m^3)
C_v	Soil coefficient of consolidation
D	Diameter (m)
E	Young's modulus (Pa)
F	Force (N)
F_e	Effective axial force (N)
F_w	Axial force on pipe wall (N)
j	Electrical current density (A/m^2)
$k_{\sigma e}$	Electrical conductivity (S/m)
k_{eo}	Electro-osmotic permeability (m^2/Vs)
k_w	Hydraulic conductivity (m/s)
L	Length (m)
L_0	Original length (m)
m_v	Soil coefficient of volume change

p_e External pressure (Pa)

p_i Internal pressure (Pa)

S_u Undrained shear strength, (Pa)

t Time (s)

u Pore water pressure (Pa)

u_e Excess pore water pressure (Pa)

v Velocity (m/s)

$\overline{v}$ Relative velocity (m/s)

υ' Pipe Poisson ratio

υ Soil Poison ratio

v^s Soil particle velocity (m/s)

z Elevation (m)

α Coefficient of thermal expansion

β Intermittent power supply

γ_w Unit weight of soil (N/m^3)

σ Total stress (Pa)

σ' Effective stress (Pa)

θ Temperature ($C°$)

ϕ Electric potential (V)

References

Al-Hamdan, A. Z., and Reddy, K. R. (2008). "Electrokinetic Remediation Modeling Incorporating Geochemical Effects." *Journal of Geotechnical and Geoenvironmental Engineering*, 134(January), 91–105.

Altaee, A., and Fellenius, B. H. (1996). "Finite Element Modeling of Lateral Pipeline-Soil Interaction." *114th International Conference on Offshore Mechanics and Arctic Engineering, OMAE 96*, Florence, Italy, 283–300.

Ansari, Y., Kouretzis, G. P., and Sheng, D. (2014). "An effective stress analysis of partially embedded offshore pipelines:

Vertical penetration and axial walking." *Computers and Geotechnics*, 58(May), 69–80.

Aubeny, C. P., Shi, H., and Murff, J. D. (2005). "Collapse Loads for a Cylinder Embedded in Trench in Cohesive Soil." *International Journal of Geomechanics*, 5(4), 320–325.

Bai, Q., and Bai, Y. (2014). "Lateral Buckling and Pipeline Walking." *Subsea Pipeline Design, Analysis, and Installation*, 221–253.

Ballard, J. C., Brier, C. De, Stassen, K., and Jewell, R. a. (2013). "Observations of pipe-soil response from in-situ measurements." *Proc. Offshore Technology Conference*, Offshore Technology Conference, Houston, Texas, 6–9.

Ballard, J., and Falepin, H. (2009). "Towards more advanced pipe-soil interaction models in finite element pipeline analysis." *Proceedings of the SUT Annual Conference*, Society of Underwater Technology, Perth, Western Australia, 1–5.

Bjerrum, L., Moum, J., and Eide, O. (1967). "Application of Electro-Osmosis to a Foundation Problem in a Norwegian Quick Clay." *Géotechnique*, 17(3), 214–235.

Bruton, D., Bolton, M., Carr, M., and White, D. (2008). "Pipe-Soil Interaction during Lateral Buckling and Pipeline Walking — The SAFEBUCK JIP." *Proceedings of Offshore Technology Conference*, Offshore Technology Conference, Houston, Texas, 20pp.

Bruton, D., White, D. J., and Cheuk, C. Y. (2006). "'Pipe/soil interaction behavior during lateral buckling, including large-amplitude cyclic displacement tests by the safebuck JIP.'" *Offshore Technology Conference*, 1–10.

Burnotte, F., Lefebvre, G., and Grondin, G. (2004). "A case record of electroosmotic consolidation of soft clay with improved soil–electrode contact." *Canadian Geotechnical Journal*, 41(6), 1038–1053.

Callister, W. D., and Rethwisch, D. G. (2014). *Materials science and engineering : an introduction*. *Wiley*, John Wiley & Sons.

Carneiro, D., and Castelo, A. (2011). "Walking analyses of HP/HT pipelines with sliding end structures using different FE models." *Rio Pipeline 2011*, Rio Pipeline Conference & Exposition, Rio de Janeiro, Brazil, 1–11.

Carr, M., Sinclair, F., and Bruton, D. (2008). "Pipeline Walking--Understanding the Field Layout Challenges and

Analytical Solutions Developed for the Safebuck JIP." *SPE Projects Facilities & Construction*, Society of Petroleum Engineers, 3(3), 1–9.

Casola, F., El-chayeb, A., Greco, S., and Carlucci, A. (2011). "Characterization of Pipe Soil Interaction and Influence on HPHT Pipeline Design." *International Society of Offshore and Polar Engineers*, 8, 111–121.

Cormie, P., McBride, J. M., McCaulley, G. O., Jensen, A., and Lidell, E. (2009). "The influence of body mass on calculation of power during lower-body resistance exercises." *Journal of strength and conditioning research / National Strength & Conditioning Association*, 16(4), 1042–1049.

Dassault Systèmes. (2014). *Abaqus analysis user's guide*. Dassault Systèmes Simulia Corporation, RI, USA.

Dingle, H. R. C., White, D. J., and Gaudin, C. (2008). "Mechanisms of pipe embedment and lateral breakout on soft clay." *Canadian Geotechnical Journal*, 45(5), 636–652.

Dutta, S., Hawlader, B., and Phillips, R. (2014). "Finite element modeling of partially embedded pipelines in clay seabed using Coupled Eulerian-Lagrangian method." *Canadian Geotechnical Journal*, 72(February 2014), 1–15.

Engineering Toolbox. (2015). "Conductivity of some common materials and gases." *http://www.engineeringtoolbox.com/thermal-conductivity-d_429.html*, <http://www.engineeringtoolbox.com/thermal-conductivity-d_429.html> (Mar. 2, 2015).

Esrig, M. (1968). "Pore pressures, consolidation, and electrokinetics." *Journal of the Soil Mechanics and Foundations Division*, Vol 94(No SM4), 899−921.

Eton, G. E. (2011). "Mitigation against lateral buckling and axial walking of subsea pipeline." Doctor of Philosophy thesis, Institute of Resilient Infracstructure, School of Civil Engineering, University of Leeds.

Hansen, E. J., and Saouma, V. E. (1999). "Numerical simulation of reinforced concrete deterioration: Part II–steel corrosion and concrete cracking." *ACI Materials Journal*, Citeseer, 96(3), 331–338.

HU, L., and WU, H. (2014). "Mathematical model of electro-osmotic consolidation for soft ground improvement." *Géotechnique*, 64(2), 155–164.

Jones, C., and Glendinning, S. (2006). "Soil consolidation and strengthening using electrokinetic geosynthetics–concepts

and analysis." *Geosynthetics*, (2), 411–414.

Joshua, H. N., and Kara, F. (2018). "Numerical study of electro-osmotic consolidation effect on pipe-soil interaction." *Applied Ocean Research*, 74, 11–27.

Lewis, R., and Humpheson, C. (1973). "Numerical analysis of electroosmotic flow in soils." *Journal of the Soil Mechanics and Foundations Division, ASCE*, Vol 95(No 4), 603−616.

Lo, K. Y., Micic, S., and Shang, J. Q. (1999). "Electrokinetic Strengthening of Soft Marine Clays." *Proceedings of the Ninth (1999) International Offshore and Polar Engineering Conference*, International Society of Offshore and Polar Engineers, Brest, France, 1–6.

Lo, K. Y., Micic, S., Shang, J. Q., Lee, Y. N., and Lee, S. W. (2001). "Electrokinetic strengthening of a marine sediment using intermittent current." *Canadian Geotechnical Journal*, 38(2), 287–302.

Merifield, R. S., White, D. J., and Randolph, M. F. (2009). "Effect of Surface Heave on Response of Partially Embedded Pipelines on Clay." *Journal of Geotechnical and Geoenvironmental Engineering*, 135(6), 819–829.

Merifield, R., White, D. J., and Randolph, M. F. (2008). "The ultimate undrained resistance of partially embedded pipelines." *Géotechnique*, 58(6), 461–470.

Micic, S., Lo, K. Y., and Shang, J. Q. (2004). "Increasing load-carrying capacities of offshore foundations in soft clays." *Journal of Petroleum Technology*, 56(2), 53–55.

Micic, S., Shang, J. Q., and Lo, K. Y. (2002). "Electrokinetic strengthening of marine clay adjacent to offshore foundations." *International Journal of Offshore and Polar Engineering*, 12(1), 64–73.

Micic, S., Shang, J. Q., and Lo, K. Y. (2003). "Electrocementation of a marine clay induced by electrokinetics." *International Journal of Offshore and Polar Engineering*, 13(4), 308–315.

Mitchell, J. K. (1960). "Components of Pore Water Pressure and Their Engineering Significance." *Clays and Clay Minerals*, 9(1), 162–184.

Mitchell, J. K., and Soga, K. (2005). *Soil Composition and Engineering Properties*. *Fundamentals of Soil Behavior (3rd Edition)*, John Wiley & Sons.

Muthukrishnan, S., Kodikara, J., and Rajeev, P. (2011). "Numerical modelling of undrained vertical load- displacement behaviour of offshore pipeline using coupled analysis." *2011 Pan-Am CGS Geotechnical Conference*, 1–8.

Oliphant, J., and Maconochie, A. (2006). "Axial Pipeline-Soil Interaction." *International Society of Offshore and Polar Engineers*, International Society of Offshore and Polar Engineers, San Francisco, California, USA, 100–107.

Perinet, D., and Simon, J. (2011). "Lateral Buckling and Pipeline Walking Mitigation in Deep Water." *Offshore Technology Conference*, (May), 2–5.

Randolph, M. F., and House, A. R. (2001). "The complementary roles of physical and computational modelling." *International Journal of Physical Modelling in Geotechnics*, Thomas Telford-ICE Virtual Library, 1(1), 1–8.

Randolph, M. F., and White, D. J. (2008). "Pipeline Embedment in Deep Water: Processes and Quantitative Assessment." *Proceedings of Offshore Technology Conference (OTC)*, Offshore Technology Conference, Houston, Texas, 1–16.

Rittirong, A., and Shang, J. Q. (2008). "Numerical analysis for electro-osmotic consolidation in two-dimensional electric field." *Eighteenth (2008) International Offshore and Polar Engineering Conference*, 8, 566–572.

Rong, H., Inglis, R., Bell, G., Huang, Z., Chan, R., and Kenny, J. P. (2009). "Evaluation and Mitigation of Axial Walking with a Focus on Deep Water Flowlines." *Proc. Offshore Technol. Conf., Houston, TX, OTC 19862*, Offshore Technology Conference, Houston, Texas, 1–10.

Staff, J. (1998). "In-Situ Casing Consolidation by Electrokinetic Methods." *Petroleum Technology*, Society of Petroleum Engineers, 50(02), 51–53.

Vermeer, P., A., and Verruijt, A. (1981). "An Accuracy Condition for Consolidation by Finite Elements." *International Journal for Numerical and Analytical Methods in Geomechanics*, 5(January), 1–14.

Virkutyte, J., Sillanpaa, M., and Latostenmaa, P. (2002). "Electrokinetic soil remediation - Critical overview." *Science of the Total Environment*, 289(1–3), 97–121.

Wan, T., and Mitchell, J. (1976). "Electro-osmotic consolidation of soils." *Journal of the Soil Mechanics and Foundations Division, ASCE*, Vol 102,(No GT5), 473−491.

Westgate, Z. J. ., White, D. J. ., Randolph, M. F. ., and Brunning, P. . (2010a). "Pipeline laying and embedment in soft

fine-grained soils: Field observations and numerical simulations." *Proceedings of the Annual Offshore Technology Conference*, 1(1), 326–340.

Westgate, Z. J., Randolph, M. F., White, D. J., and Li, S. (2010b). "The influence of sea state on as-laid pipeline embedment: A case study." *Applied Ocean Research*, 32(3), 321–331.

Wu, H., Wu, W., and Hu, L. (2012). "Numerical model of electro-osmotic consolidation in clay." *Géotechnique*, 62(6), 537–541.

Yuan, J., and Hicks, M. A. (2015). "Numerical analysis of electro-osmosis consolidation: a case study." *Géotechnique Letters*, 5(July–September), 147–152.

Yuan, J., Hicks, M. a, and Jommi, C. (2015). "Large strain consolidation of clays : Numerical comparison between evaporation and electro-osmosis dewatering." *Computer Methods and Recent Advances in Geomechanics*, (1990), 1655–1660.